



## RESEARCH ARTICLE

### Histomorphometric Comparison of Canine and Feline Nictitating Membranes

Gashaw M Ali<sup>1</sup>, Othman J Ali<sup>2</sup>, Snur MA Hassan<sup>1\*</sup> and OI Dana<sup>2</sup>

<sup>1</sup>Department of Anatomy and Pathology, College of Veterinary Medicine, University of Sulaimani, 4601, KRG/Iraq;

<sup>2</sup>Department of Surgery and Theriogenology, College of Veterinary Medicine, University of Sulaimani, Sulaymaniyah, 4601, KRG/Iraq.

\*Corresponding author: snur.amin@univsul.edu.iq; hassan\_snur@yahoo.com

#### ARTICLE HISTORY (23-034)

Received: January 21, 2023  
Revised: May 22, 2023  
Accepted: May 26, 2023  
Published online: June 10, 2023

#### Key words:

Anatolian shepherd dog  
Feral cat  
Masson trichrome  
Nictitating membrane  
Verrhof Van Gieson

#### ABSTRACT

The nictitating membrane is a conjunctival fold, located at the medial canthus of the eyes, it serves to maintain healthy eyes in domestic animals. This study was conducted on 40 nictitans glands and cartilages, obtained from 20 clinically healthy local Anatolian Shepherd dogs and 20 Feral cats. The nictitans membranes were dissected, and macerated using Potassium hydroxide (KOH), and then the cartilage tissue was stained with Alcian blue stain. The samples were fixed in 10% neutral buffer formalin for histological purposes and then prepared for H&E, Verhoeff's-Van Gieson, and Masson trichrome stains. ImageJ analyzer and AmScope™ were used for anatomical and histological morphometrics respectively. The morphometric analysis revealed a significant difference in the cartilage morphometric dimensions between dogs and cats in correlation to their ages and weights. Both species showed a medium to strong positive correlation, but in the dogs, the cartilage body width had a low positive correlation with age and weight. The histomorphometric study of both species for the acini, interlobular septa, intralobular septa, intralobular duct, chondrocyte number, and the capsule was a significant ( $P > 0.05$ ) variable between species and among different groups also. We conclude that the nictitans cartilage in dogs was longer and narrower vs. to the cats, and their nictitans gland was horizontally oval-shaped while vertically oval-shaped in the cat. The nictitans gland in the dogs was composed of compound tubuloacinar serous cells that were supported by hyaline cartilage, whereas the nictitans gland in the cats was made up entirely of compound acinar units with elastic cartilage.

**To Cite This Article:** Ali GM, Ali OJ, Hassan SMA, Dana OI, 2023. Histomorphometric comparison of canine and feline nictitating membranes. Pak Vet J, 43(3): 412-420. <http://dx.doi.org/10.29261/pakvetj/2023.042>

#### INTRODUCTION

Companion animals like the dog and cat and more specifically the dog, provide an untapped resource for translational research in the biomedical sciences (Kol *et al.*, 2015). Integrating canine and feline subjects into preclinical studies can speed up and improve the framework in which research is translated to the human clinic and ultimately lead to discoveries that will improve the health of humans and animals. Unlike traditional laboratory animals (e.g., rabbits, mice, rats), naturally-occurring diseases in dogs better reflect the complex genetic, environmental and physiological background present in humans (Garden *et al.*, 2018; Partridge and Rossmeisl Jr, 2020). Despite the paucity of comparative ophthalmology literature, veterinarians routinely evaluate pets to diagnose and treat a variety of ocular disorders, drawing on the knowledge of general practitioners and

veterinary experts around the world. Importantly, many canine ocular diseases have striking similarities in phenotype to their clinical human counterparts, as seen by keratoconjunctivitis sicca (often known as "dry eye"), they might so act as spontaneous animal models of eye illnesses (Hoffman and Dow, 2016).

The nictitating membrane is a modified conjunctival fold that protrudes from the medial canthus of the eyes in domestic (König *et al.*, 2007) and wild animals including red kangaroo (Klećkowska-Nawrot *et al.*, 2016), koala (Kempster *et al.*, 2002), bear (Klećkowska-Nawrot *et al.*, 2019), roe deer (Klećkowska-Nawrot *et al.*, 2013) and wild ruminant (Al-Ramadan and Ali, 2012), as well as in many other vertebrates including sharks (Collin, 2018), amphibians (Keller and Shilton, 2002), reptiles and birds (Schobert *et al.*, 2013). The nictitating membrane is covered by non-keratinized stratified squamous epithelium with an underlying stroma of fibrous connective tissue that

contains glandular, lymphoid, and elastic tissues (Park *et al.*, 2016). The nictitating membrane is structurally supported by T-shaped flat cartilage, consisting of a long narrow appendix with a short crossbar end, that determines the shape of the third eyelid (Paszta *et al.*, 2021). Nictitans gland is defined as a holocrine gland, also called the superficial gland's third eyelid (SGTE) or anterior gland of the third eyelid (AGTE), it is oval-shaped and located on the medial canthus of the eye at the base of the cartilage, within the third eyelid between medial rectus muscle and the ventral rectus muscle of the eyeball, and is partly protected by the ventral oblique muscle (Ofri *et al.*, 2008). The duct of this gland typically opens on the medial (corneal) surface of the nictitating membrane (Kumar, 2015). The primary function of this gland is to flush foreign bodies and micro-organisms from the eyeball and supply the cornea with nutrients, including oxygen, amino acid, vitamin A, growth factor, and antibodies (Park *et al.*, 2016).

Dogs and cats possess only a single type of nictitans gland (there are other periorbital glands) but some species such as birds, possess a deeper gland that is referred to as the Harderian gland (Cooper, 2010). The nictitans gland is a seromucous gland that produces watery and mucous secretions that are protecting the eyes from dryness (Paszta *et al.*, 2021).

The absence of canine and feline research for translational objectives is mostly attributed to perceived barriers including a lack of transgenic dogs and cats and inadequate molecular resources compared to laboratory animals (Barabino and Dana, 2004; Pennington *et al.*, 2017). The lack of non-invasive experimental models to mimic disease pathophysiology in this species, in addition to the scarcity of information on the anatomy and histology of the ocular surface in pet animals, are, in the authors' opinion, more scientifically significant barriers to using dogs and cats in ophthalmology research. Due to significant species differences in ocular anatomy and physiology, straightforward extrapolation from other animals is unfortunately not possible (Vézina, 2013; Gilger *et al.*, 2014).

The presence of nictitans membrane with their associated structures are very important for the maintenance of healthy eyes, and for this reason, we aimed to explore the anatomical and histological configurations of the nictitans cartilage and gland with their age-related morphometric alterations in Anatolian shepherd dog and feral cat.

## MATERIALS AND METHODS

**Animals:** The study was conducted on twenty Anatolian shepherd dogs (10 males and 10 females) and twenty feral cats (10 males and 10 females) of different ages and weights admitted to the veterinary teaching hospital, college of veterinary medicine, the University of Sulaimani during September 2021 to October 2022 due to the car or other accidents for clinical inspection and post-mortem findings.

**Ethical approval:** This study was approved by the Veterinary College Research Ethics Committee (VREC, 030510), University of Sulaimani, based on CONCEA (National Animal Experiment Control Council) ethical norms for animal experimentation.

**Study design:** According to their ages and weights, the animals were categorized into three groups. In dogs; group one, group two, and group three including those samples with ages and weights ranged from (1-6 months and 1-10 kg), (6-12 months and 10-20 kg) and (above 1 year and 20-40 kg) respectively. In cats; group one, group two, and group three including samples from cats with ages and weights ranged from (1-6 months and 0.5-2.5 kg), (6-12 months and 2.5-4 kg) and (above 1 year and 4-5 kg) respectively.

**Dissection and modified maceration technique:** The cartilage and gland were carefully dissected from the nictitans membrane using a scalpel and sharp-sharp pointed scissors (Johnston and Tobias, 2017). A modified maceration technique was performed for verifying the three-dimensional form of the cartilage according to (en Murciélagos and Adultos, 2009; Mohsen *et al.*, 2013). The fresh samples of nictitans tissues were immersed in 2% potassium hydroxide for 18 hours at 40°C under visual control and careful dissection of the cartilage from the surrounding tissues.

**Alcian blue staining protocol:** After careful maceration of the third eyelid, the cartilage tissue was photographed by a camera (Nikon, Japan). The Alcian blue staining (pH=4.2) method was used for further demonstration of cartilage morphologic structures, the specimens were washed three times with distilled water (DW) and fixed in 0.15% formalin for 2-3 days (Schlegel *et al.*, 2001). Then the sample was completely immersed in a mixture of Alcian blue (10 mg 8GX) (C.I.74240 Merck, Germani) for 2 days. The Alcian blue was prepared from a mixture of Alcian blue 10 mg (0.01 g), glacial acetic acid (20 ml), and 95% ethyl alcohol (80 ml). After staining with Alcian blue, the samples were rehydrated by passing through descending concentrations of ethyl alcohol graded from 95%, 75%, 40%, and 15%, two hours per each grade, and completed by immersing it in DW for 8 hrs. Finally the samples were preserved in pure glycerin as permanent storage (en Murciélagos and Adultos, 2009; Mohsen *et al.*, 2013).

**Histologic staining:** Third eyelid samples were collected and fixed with 10% NBF then the tissues were processed through the following steps; third eyelid tissue undergo dehydration and was passed through the ascending concentration of ethanol baths by using an automatic processor as follows: 70%, 80%, 90%, and 100%, each bath for 1.5 hours, then the samples were put in three baths of xylene as a clearing agent, each bath for 10 minutes, after that the tissues were impregnated with paraffin used twice for 2 hours each time in a paraffin bath adjusted to 58 °C in a thermal oven. Then tissues were poured into a metal mold with a labeled tissue cassette of pure wax which forms a paraffinized block. They were left for 24 hours to give paraffin time to solidify, then each paraffinized block was sectioned by a manual rotary microtome in a thickness of 4µm. Then the ribbons were transferred into a water bath at 45°C. Finally, the sections were mounted on clean glass slides which in turn were dried in a thermo oven at 45°C for 24 hours (Spencer *et al.*, 2012).

**Masson's trichrome stain:** The sections were deparaffinized in xylene for 10 min, then the sections were

rehydrated by passing through a decreasing concentration of alcohol, 5 min for each concentration, and then sections were rinsed well in distilled water. Mordant formalin was used for fixing the sections in Bouin solution for 1 hour at 56°C in an oven, after that the slides were removed from the oven and allowed to cool down, then sections were washed in running water until the yellow color disappears., then after rinsing the section in distilled water all the sections were stained in Gill hematoxylin for 10 minutes and washed in running water for 10 minutes. The sections were stained in Biebrich scarlet-acid fuchsin solution for 2 minutes and then rinsed in distilled water. Subsequently, the slides were placed in phosphomolybdic/phosphotungstic acid solution for 10-15 minutes. Then the sections were stained in an aniline blue solution for 5 minutes and then rinsed the slides in distilled water, later the slides were placed in 1% acetic acid solution for 3-5 minutes. Lastly, the sections were dehydrated in ethanol and cleared with xylene and finally mounted with a cover slip (Sheehan and Hrapchak, 1980).

**Verhoeff's-Van gieson stain:** The sections were deparaffinized in xylene for 10 min. Then sections were rehydrated by passing through a decreasing three concentrations of alcohol, 5 min for each concentration, and then sections were rinsed well in distilled water, subsequently, the sections were placed in Verhoeff's elastic tissue stain for 1 hour and the sections were washed 2 times in distilled water. After that, the sections were differentiated microscopically in 2% ferric chloride until the elastic fibers were distinct and the background was colorless to light gray, and the sections were rinsed in distilled water. Then the sections were placed in sodium thiosulfate for 1 minute and then washed in running tap water for 5 minutes. Later the sections were counterstained in van Gieson stain for 1 minute and differentiated in 95% alcohol. Finally, the sections were dehydrated in absolute alcohol, cleared in xylene, mounted, and lastly, the sections were covered and slipped (Sheehan and Hrapchak, 1980).

**Gross morphometric and ImageJ evaluation:** Digital photographs were taken for all the samples of nictitans cartilage and the glands with built-in stainless Caliper. ImageJ (developed by the National Institute of Health and the Laboratory for Optical and Computational Instrumentation) was used for measuring the cartilage dimensions including cartilage's heights, widths, thickness, dorsal wing, and ventral wing, as well as the nictating gland's heights, widths and the thickness (Fig. 1).

The measurement was performed on the ruler-calibrated images. Initially, the image was dragged into the ImageJ software, and then the straight-line selection tool was used to drag a line across the calibrated ruler on the image to specify a distance (e. g. 100µm). Then, setting the scale by clicking the Analyze tool, the set scale window was opened that show the length of the dragged line in pixels (e.g. 1000 pixel). Then this specified distance in pixels (1000 pixels) that was determined by the freehand tool on the calibrated ruler was converted into a meter distance on the image (e.g. 1000 µm) (Fig. 3). From the ImageJ toolbar, the measuring tool was selected to determine the length of the selected part of the cartilage or the gland in all the groups.

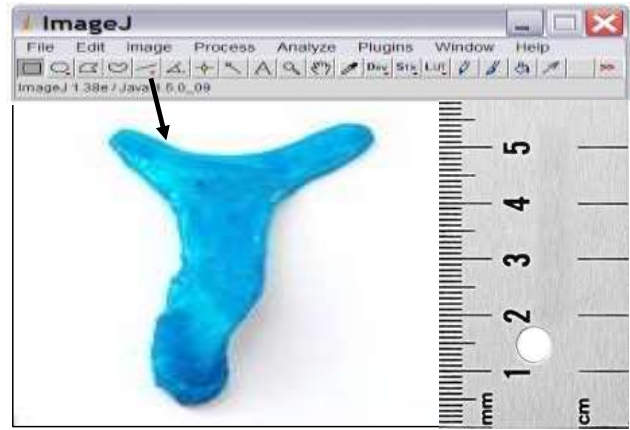


**Fig. 1:** Measuring the dimensions of the nictitans cartilage and the glands using ImageJ on the maceration samples stained with Alcian blue. After setting the scale, the straight-line tool was selected to measure the length of the dimensions (Black arrow). By selecting the measure tool from the Analyze toolbar the length of each part of the cartilage and the glands were explored in a new window.

**Histomorphometric assessment of nictitans gland and cartilage:** Under a light microscope, all the histological sections which were stained by H&E and special stains were examined and the measurement thickness for the following histologic structures was taken by (Amscope™, Japan) software such as; capsule, lobe diameter, intra with interlobular septa, and cartilage, for each section 5 randomly chosen sections at 100X magnification. The alveolar/acinar and tubular thickness was measured at 400x magnification of 10 randomly chosen fields in each section of each species for both H&E and special stain. For the chondrocytes counting, the special stained section at 400x magnification was photomicrographed and divided by a grid into 15 squares, and the mean number for each group was calculated.

**Statistical analysis:** Statistical analysis, bar charts, and lines of correlation were performed with SPSS statistics version 24 (IBM, SPSS Inc, Chicago, USA). A p-value < 0.05 was considered statistically significant. The Shapiro-Wilk test was used to test the normality of the data. Data were analyzed by two-way ANOVA evaluating the effect of both species and different ages and sex, followed by multiple comparisons with the Duncan test. To determine the correlation between groups the Pearson's coefficient (r) correlation was used.

## RESULTS

**Anatomical study:** The cartilages of the macerated samples were strongly colored with Alcian blue and showed a long-straight crossbar that held the dorsal and the ventral wing at the free end. The nictitans cartilages were T-shaped, consisting of three borders and two surfaces; the medial border curved and parallel with the nose, then the dorsal and ventral borders were straight and parallel to the upper and lower eyelid. The surfaces were surrounded by connective tissue, which was diverted into the palpebral and the bulbar surfaces. The nictitans cartilage was composed of a long-straight crossbar, holding dorsal and ventral wings at the free end. The dorsal wing was directed dorsally and it was slightly longer and curved than the ventral wing. The nictitans gland appeared as a uniform, undivided, oval-shaped structure located at the base of the

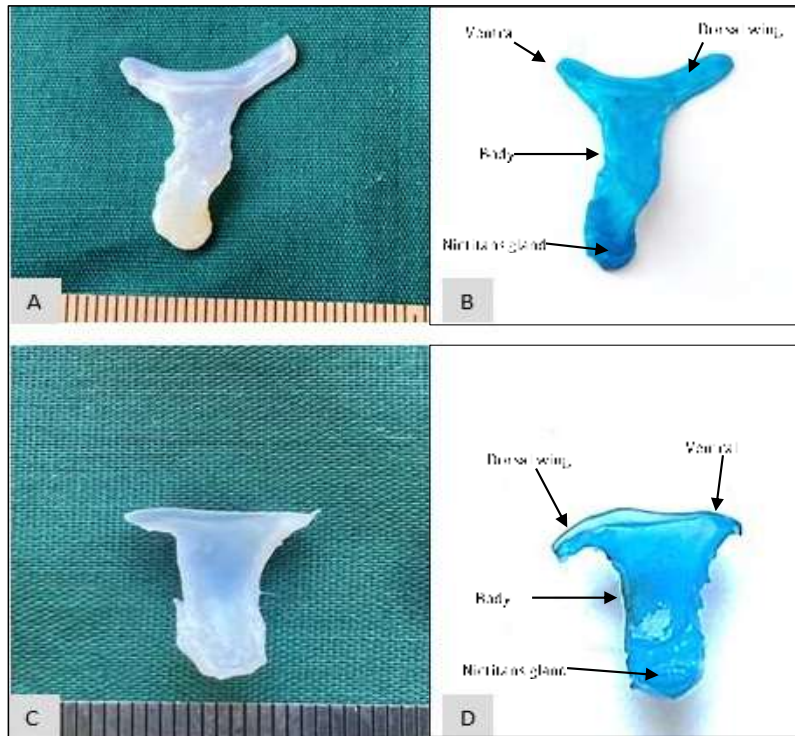


**Fig. 2:** Shows T-shaped cartilage using KOH maceration technique and their staining with Alcian blue in the dog (A and B) at the palpebral surface, and cat (C and D) at the corneal surface.

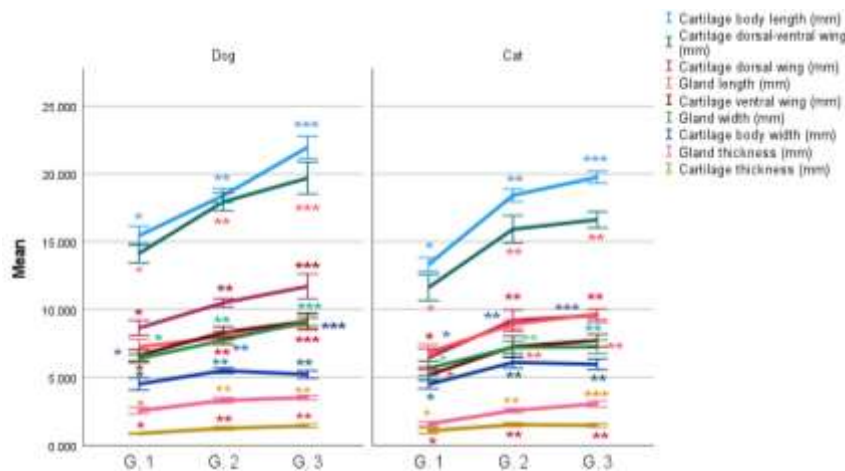


**Fig. 3:** The morphometric analysis of the nictitans cartilage and glands in dogs and cats according to their age and weight (mm) (Mean  $\pm$  SE), using (Two-way ANOVA). Groups are mean of age and weight-related for example in dogs, G1; aged (1-6 months) and weighted (1-10 kg), G2; aged (6-12 months) and weighted (10-20 kg), and G3; aged (more than 12 months) and weighted (over 20 kg). In cats, G1; aged (1-6 months) and weighted (0.5-2.5 kg), G2; aged (6-12 month) and weighted (2.5-4 kg), and G3; aged (more than 12 months) and weighted (4-5 kg).

cartilage cross bar between the medial and the ventral straight muscles and was partially covered by the ventral oblique muscles (Fig. 2).

**Morphometric analysis:** In morphometric analysis, it was found that there were no significant differences in the morphometric configuration between males and females, as well as, between the right and the left side of the eyes in both species. However, it was found that there was a significant difference in the cartilage morphometric dimensions between dogs and cats. Dogs had greater cartilage body length than cats, particularly in G1 and G3 ( $P > 0.05$ ), but no significant differences were found in the cartilage body length in G2 between dogs and cats ( $P < 0.95$ ). For the cartilage body width, it was recorded that cats had wider cartilage than dogs, particularly in G2 and G3, were showed significant differences ( $P > 0.05$ ), while G1 showed no significant differences in the cartilage body width between dogs and cats ( $P > 0.05$ ). Moreover, a significant difference was found in the cartilage thickness in cats in G1 and G2 when compared to the dogs ( $P > 0.05$ ), but no significant differences were

recorded in G3 between both species ( $P > 0.05$ ). The lengths of the dorsal-ventral wing, dorsal wing, and ventral wing were longer in the dogs in G1, G2, and G3 when compared to the cat but statistically, they were not significant ( $P > 0.05$ ) (Fig. 3).

The nictitans gland morphometric measurements showed longer dimensions in a cat when compared to the dogs, particularly in G2 and G3 ( $P > 0.05$ ). However, no significant differences were recorded in the gland length in G1 in both species ( $P > 0.05$ ). Moreover, there was a significant difference in the gland width between dogs and cats, dogs had wider nictitans glands than the cats in G1 and G3 ( $P > 0.05$ ), however, no significant differences were found in G2 between dogs and cats ( $P > 0.05$ ) (Fig. 3). Further, it was found that dogs have thicker nictitans glands than cats ( $P > 0.05$ ). Interestingly, there were no significant differences in the eye diameter between the dogs and the cats ( $P > 0.05$ ). Concerning the cross-correlation of these parameters with age and weight-related, they had a medium to strong positive correlation in both species, but in the dogs, the cartilage body width had a low positive correlation with age and weight (Fig. 3).

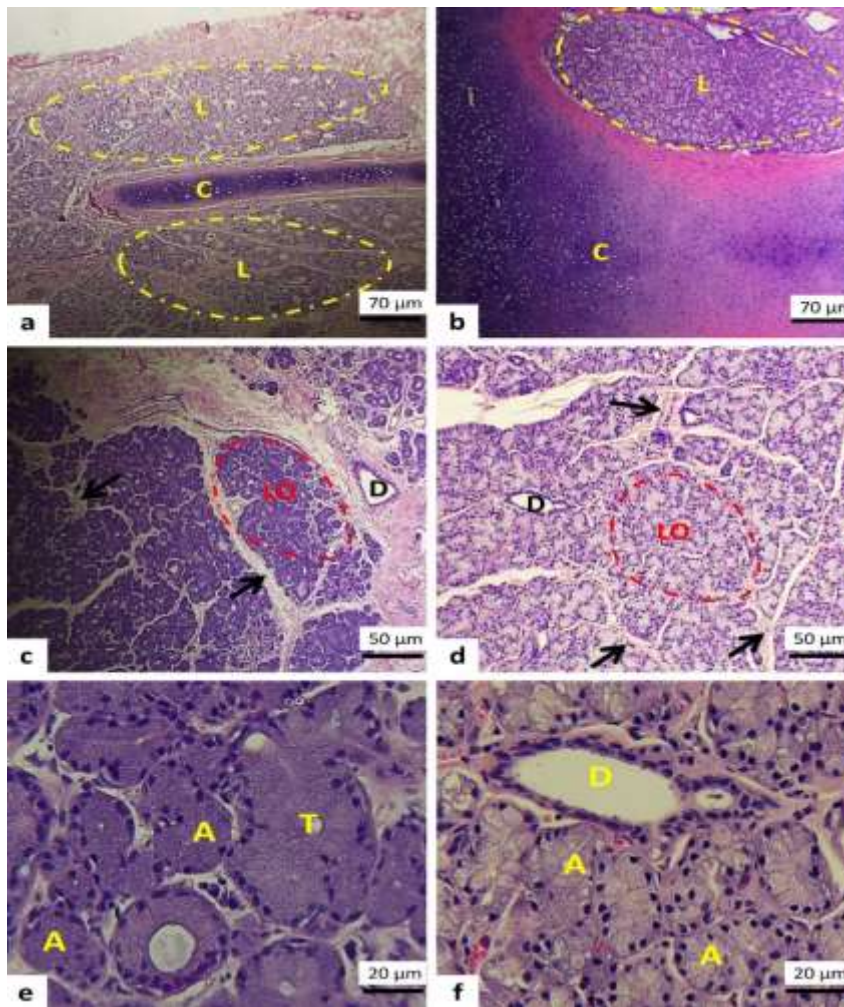


**Fig. 4:** Microscopic section of the nictitans membrane revealed; a,c,e: Compound tubulo acinar nictitans gland parenchyma that supported by the hyaline cartilage, and trabeculae (black arrow) that divided the parenchyma into lobe and lobules in the dog. b,d,f: Presence of elastic cartilage that support the compound acinar nictitans gland parenchyma, and trabeculae (black arrow) that divide the organ into lobe and lobules in cat. C: capsule, L; Lobe, LO; lobules, C: cartilage, A; acini, T; tubule, D: Duct (H&E stain).

**Histo-morphometric evaluation:** Histological features of the nictitans gland in dogs are characterized by a compound tubuloacinar serous gland that surrounded the hyaline cartilage shaft of the third eyelid (Fig. 4a and 5a) respectively in comparison to the cats that is composed of a compound acinar gland that is supported by a thin layer of connective tissue capsule, enriched of elastic fiber (Fig. 4b and 5b) correspondingly. In both species, the connective tissue from the capsule sends trabeculae and divide the glandular parenchyma into lobe and lobules that are surrounded by thick and thin interlobular septa (Fig. 4c,d, and Fig. 5c-f). The glandular parenchyma in dogs is seromucous secretory acini (Fig. 4c,e and 5c,e), whereas the tubular acini less predominate vs. serous acini in comparison to cat species in which glandular parenchyma that composed of only serous acini (Fig. 4d,f and Fig. 5d,f), the serous acini showed small lumen with a spherical shape of one-row pyramidal cells and an oval, peripheral nucleus near the basement membrane with eosinophilic cytoplasm. While the tubules revealed a wide, irregular lumen composed of a single layer of tall cells, with oval nuclei located in the basal area of each cell, and pale vacuolated cytoplasm.

The microscopic structure of hyaline cartilage in a dog's third eyelid is composed of huge numbers of oval-spherical-shaped single chondrocytes with a few isogenic groups that are arranged as 2 chondrocytes and a high amount of extracellular matrix in the dog (Fig. 5g) vs. cat in which the third eyelid was surrounded by typical elastic

cartilage with oval-shaped chondrocytes mostly seen as an isogenous group vs. to those found in a dog (Fig. 5h).

In the histo-morphometric assessment of the superficial gland and the third eyelid cartilage in dogs and cats, significant differences were found among various ages in cat and dog species in which lobe thickness increased in aged species ( $P>0.05$ ), while the dog had a significantly larger lobe thickness in all aged groups vs. cat species of similar ages ( $P>0.05$ ). Regarding the acini thickness, there were no significant differences between dog and cat ( $P>0.05$ ), only a significant difference ( $P>0.05$ ) was found in group G2. In addition, the intralobular duct thickness had significant differences among all age groups in cats and dogs, whereas each group in dogs had significantly greater intralobular duct thickness vs. the same age group in cats ( $P>0.05$ ). Concerning, the tubular diameter, which was found only in the dogs, and absent in the cat, showed no significant differences ( $P>0.5$ ) among the dog's age groups (Fig. 6).

The morphometric analysis regarding the average thickness of the interlobular septa in dogs and cats in G1, G2, and G3 revealed that the interlobular septa had highly significant differences between all the groups in dogs and cats, whereas dogs showed thicker interlobular septa with significant differences vs. cats in G1 ( $P>0.05$ ), while G3 showed no significant differences ( $P>0.5$ ). Furthermore, no significant differences were seen regarding intralobular septa in both species in G3 ( $P>0.5$ ) except for G2 in the dog and G1 in cats showed thicker intralobular septa ( $P>0.05$ ).

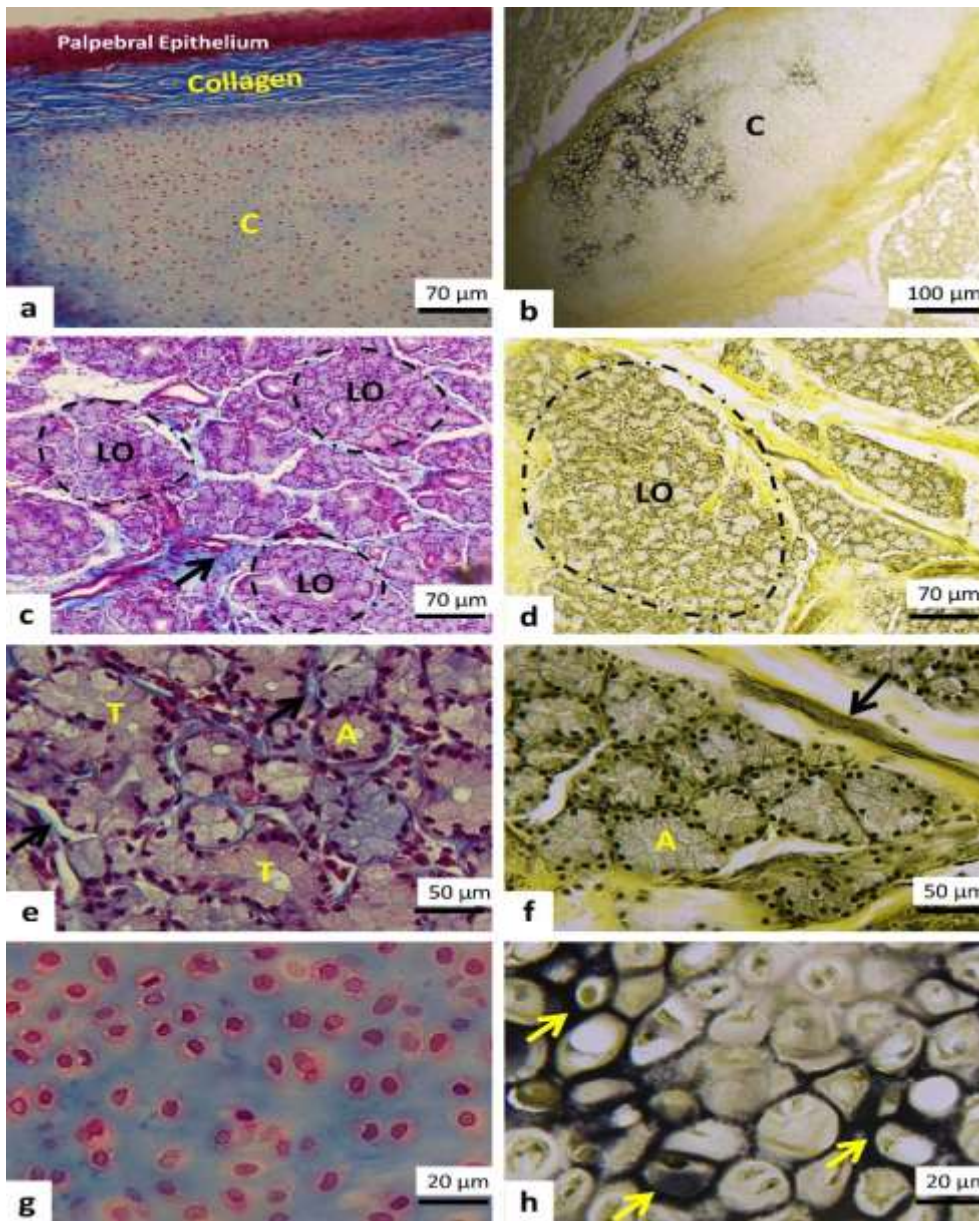


**Fig. 5:** Microscopic section of the nictitans membrane showed; a; Nictitans cartilage that is composed of hyaline cartilage and surrounded by collagenous connective tissue in the dogs (Trichrome stain). b; Nictitans cartilage is composed of elastic cartilage and surrounded by elastic connective tissue in the cats (Van Gieson elastic stain). c and e; Compound tubulo acinar gland in the dogs (Trichrome stain). d and f; Acinar gland that surrounded by elastic fiber (black arrow) in the cats (Van Gieson elastic stain). g; Oval-spherical more single chondrocytes in the dogs (Trichrome stain). h; Large numbers of isogenous grouped chondrocytes with elastic fiber (yellow arrows) in the cats, C; capsule, LO; lobules, C; cartilage, A; acini, T; tubule.

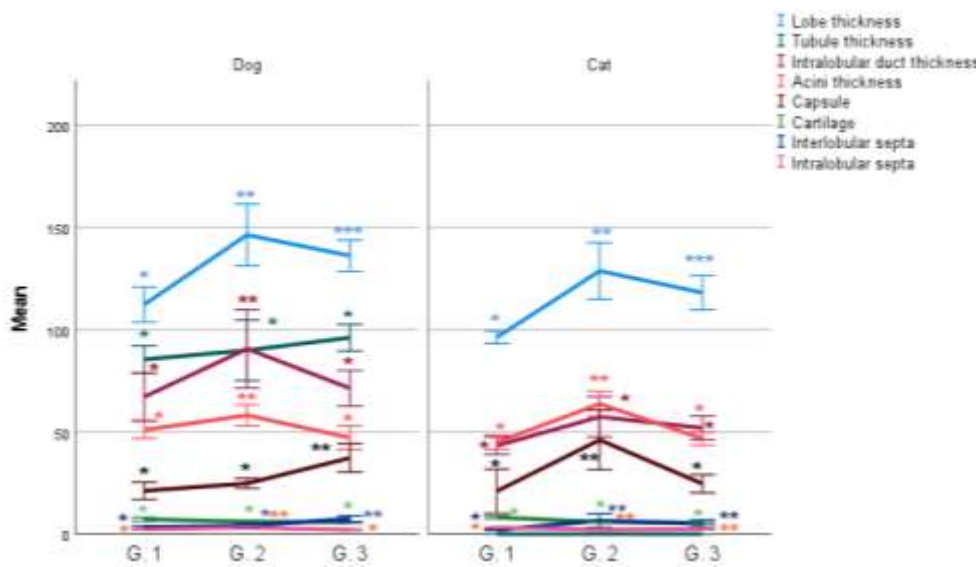


**Fig. 6:** The histomorphometric correlation of different histological structures of the nictitans gland and cartilage in dogs and cats according to their age and weight ( $\mu\text{m}$ ) (Mean  $\pm$  Standard error), using (Two-way ANOVA).

Relating the thickness of the gland capsule had significant differences ( $P > 0.5$ ) in G3 in dogs and G2 in cats, while other groups showed no significant differences ( $P > 0.5$ ).

Interestingly, the morphometric analysis of chondrocytes within each group of dogs and cats and between each species showed no significant differences ( $P > 0.5$ ) (Fig. 6).

## DISCUSSION

Over the preclinical models of ocular surface disease currently in use, dogs and cats have a few benefits. Compared to laboratory rats or rabbits, their ocular anatomy is more similar to humans (Awwad *et al.*, 2017), and both species experience spontaneous disorders (such as herpes keratitis and dry eye disease), which have a striking resemblance to human pathologies (Gelatt *et al.*, 2006; Ledbetter *et al.*, 2018). Therefore, this study focused on the anatomic-histologic detail structure of canine and feline nictitating membranes that help in understanding the better relationship between them and choosing the best animal model to study in human ophthalmology.

The nictitating membrane, sometimes known as the subconjunctival gland or intra-orbital gland, is a prominent semilunar conjunctival fold. It is situated naso-ventrally of the eyelid in dogs and cats, resembling that of elasmobranch fish, amphibians, reptiles, birds, and mammals (except humans) (Murphy *et al.*, 2012; Park *et al.*, 2016; Carvalho *et al.*, 2020), as well as, it was previously described in the literature in the other canines species (Lantyer-Araujo *et al.*, 2019). The aqueous component of the tear film in dogs is made up of varying amounts of contributions from the nictitating membrane gland and the orbital lacrimal gland (Gilger *et al.*, 2022). In actuality, rabbits' tears flow far more slowly than those of humans (Davies, 2000), a differential that is most likely explained by variations in blink rate, mucin composition, and tear film stability (Oriá *et al.*, 2018). Since the time it takes for the tear fluid to replenish in humans and dogs and cats is about the same (5-10 min), these differences would be minimized when working with companion animals (Davies, 2000).

Macroscopically, the marginal part of the third eyelids was thick and pigmented in Anatolian Shepherd dogs and Feral cats. The cartilage of the nictitans membrane in both species was T-shaped and composed of a long straight crossbar, holding a long curved dorsal wing and the ventral wing, these features are similarly reported in the other breeds of dogs (Paszta *et al.*, 2021), crab-eating fox, the maned wolf (Lantyer-Araujo *et al.*, 2019; Carvalho *et al.*, 2020), and domestic cats in Lubeck town of Germany (Schramm *et al.*, 1994). Interestingly, it was found that the nictitans glands in Anatolian Shepherd dogs and Feral cats have appeared as rounded, smooth, light yellowish-pink nodules. They are varied from the glands of other breeds of dogs such as captive South African painted and domestic dogs, which have light pinked oval shaped nictitans glands (Murphy *et al.*, 2012; Paszta *et al.*, 2021).

In the morphometric analysis, it was found that the average length of the cartilages in the Anatolian Shepherd dogs is longer than those of the captive dogs (Paszta *et al.*, 2021), carp-eating fox and other species of domestic dogs (Lantyer-Araujo *et al.*, 2019). In addition, the average length of the cartilage dorsal-ventral wing in Anatolian Shepherd dogs is smaller than those of female captive dogs (Paszta *et al.*, 2021). Otherwise, the average cartilage width in Anatolian Shepherd dogs is narrower than those recorded in the crab-eating fox and domestic dogs (Lantyer-Araujo *et al.*, 2019). Similarly, the dimensions of the nictitans glands were varied in both species, as well as, from the other reported literature. The average length and

width of the nictitans gland in Anatolian Shepherd dogs were smaller than those of the South African painted captive female dogs (Paszta *et al.*, 2021), as well as from crab-eating fox and other domestic dogs (Lantyer-Araujo *et al.*, 2019). However, in the latter two species (crab-eating foxes and domestic dogs), the authors did not consider sexual dimorphism (Lantyer-Araujo *et al.*, 2019). As well as, other studies recorded the greater length and width of the nictitans glands than those of our study, such as in the Pit Bull Terrier and Pointer mixed dog (Park *et al.*, 2016). Interestingly, the only difference in the size of the nictitans gland is from those of Mongrel dogs, the gland length and width were  $(1.27 \pm 0.03 \text{ mm})$  and  $(0.82 \pm 0.02 \text{ mm})$  respectively (Cabral *et al.*, 2005). In addition to the length and width, it was found that the thickness of the gland in the Anatolian Shepherd dogs was approximately similar to that of Pit Bull terrier dogs (Park *et al.*, 2016), while, it was varied from the other breeds of dogs; it was thinner than those in the female captive dogs (Paszta *et al.*, 2021), crab-eating fox and domestic dog (Lantyer-Araujo *et al.*, 2019), but it was thicker than Mongrel (Cabral *et al.*, 2005) and the Pointer Mixed breeds of dogs (Park *et al.*, 2016). In this study, it found that the nictitans cartilage parameters grew dramatically during ageing in both species; however, cartilage body width and ventral wing in Anatolian shepherd dogs increased slightly when compared to the cats. The nictitans gland length and thickness were statistically significant in that they increased slightly more in the dogs than in the cats with weight and age, whereas gland width increased considerably more in dogs than in cats. Only one of the five animals with prolapse of the nictitating membrane gland was older than a year, which is consistent with the results of the retrospective study by Mazzuchelli *et al.*, which found that prolapse was significantly more common in dogs up to that age (Mazzuchelli *et al.*, 2012).

Microscopically, this study documented also that the cartilage of the third eyelid in Anatolian Shepherd dogs was hyaline, which was similar to that of a captive female dog (Paszta *et al.*, 2021), other domestic dogs in Stuttgart town of Germany (Schlegel *et al.*, 2001), and in Mongrel dogs (Cabral *et al.*, 2005). In Feral cats, the cartilage tissue is composed of an elastic fiber which was similar to the other species such as domestic cats in Lubeck and Stuttgart town of Germany (Schramm *et al.*, 1994; Schlegel *et al.*, 2001), Equidae, lion, and Suidae in which the elastic fibers are particularly numerous, but non uniformly distributed (Barasa, 2003).

The nictitans gland was composed of a compound tubuloalveolar (seromucous) gland in dogs and a compound acinar (serous) in cats. This finding is similar to the other breeds of dog (Alexandre-Pires *et al.*, 2008), such as the Mongrel dog (Cabral *et al.*, 2005), Captive female dog (Paszta *et al.*, 2021) and domestic dogs in Darmstadt town of Germany (Cazacu, 2010; Murphy *et al.*, 2012).

The histomorphometry in Anatolian shepherd dogs showed that the diameter of acini and the tubules were larger than Captive dogs (Paszta *et al.*, 2021) and Mongrel dogs (Cabral *et al.*, 2005). The capsule thickness and interlobular septa were significantly thinner than that of the Captive dogs (Paszta *et al.*, 2021) and the interlobular connective tissue in Mongrel dogs (Cabral *et al.*, 2005). While the intralobular septa in our study of the Anatolian

shepherd dogs were thinner than those of the intralobular connective tissue in the mongrel dogs. In addition, the intralobular duct in the Anatolian shepherd dogs was larger than the intralobular duct in mongrel dogs. (Cabral *et al.*, 2005). Currently, it found that the histomorphometric study of Anatolian shepherd dog species for interlobular septa, capsule, and chondrocyte number, as well as, the morphometric assessment for the cat species of the acini, interlobular septa, intralobular septa, intralobular duct, chondrocyte number, and capsule. No other research has been done to establish the correlation between all microscopic parameters with age and weight-related in both species. Therefore, the microscopic correlation in our study in both species statistically significant in that they increased slightly during aging, while the correlation of acini in dogs, capsule in cats, and intralobular septa, chondrocyte number in both species reduced grew during aging.

**Conclusions:** This study concluded the detailed normative morphometric anatomic and histologic configuration of the nictitans gland and the cartilage that varied between Anatolian shepherd dogs and Feral cats and during aging. These findings could help the researchers to investigate alterations induced by disease status and to inform strategies for the prevention of unwanted outcomes.

**Acknowledgments:** We would like to thank the Veterinary Teaching Hospital belonging to the College of veterinary medicine, University of Sulaimani, Sulaymaniyah, Iraq, for the maintenance and support of the animal house. The animal house and the project are funded by the Ministry of Higher Education and scientific research, Kurdistan Regional Government, Kurdistan, Iraq.

**Conflict of interest:** All authors declare no conflict of interest.

**Authors contribution:** The experiment was carried out by Gashaw MA, Othman JA, and Snur MAH. Both Othman JA and Snur MAH supervised came up with the initial concept, produced the article, and double-checked the data. The paper is also written by Gashaw MA, Othman JA, and Snur MAH. OI Dana contributed to analyzing the data statistically using SPSS. The work has been read and approved by all authors.

## REFERENCES

- Al-Ramadan SY and Ali AM, 2012. Morphological studies on the third eyelid and its related structures in the one-humped camel (*Camelus dromedarius*). *J Vet Anatomy* 5:71-81.
- Awwad S, Mohamed Ahmed AH, Sharma G, *et al.*, 2017. Principles of pharmacology in the eye. *British J Pharmacol* 174:4205-23.
- Barabino S and Dana MR, 2004. Animal models of dry eye: a critical assessment of opportunities and limitations. *Invest Ophthalmol & Visual Sci* 45:1641-6.
- Barasa A, 2003. Morphology and structure of the nictitating membrane cartilage in mammals. *Morphologie* 87:5-12.
- Cabral VP, Laus JL, Dagli MLZ, *et al.*, 2005. Canine lacrimal and third eyelid superficial glands macroscopic and morphometric characteristics. *Ciência Rural* 35:391-7.
- Carvalho CM, Rodarte-Almeida AC, Beanes AS, *et al.*, 2020. Ophthalmic contributions to assessing eyes of two neotropical canids: *Cercopithecus thomasi* and *Chrysocyon brachyurus*. *Vet Ophthalmol* 23:460-71.
- Cazacu P, 2010. Researches concerning the morphology of the nictitating gland in dogs. PhD Thesis. IAȘI:1-7.
- Collin SP, 2018. Scene through the eyes of an apex predator: a comparative analysis of the shark visual system. *Clin and Exp Optometry* 101:624-40.
- Cooper S, 2010. The canine third eyelid. *UK Vet Com Anim* 15:52-7.
- Davies NM, 2000. Biopharmaceutical considerations in topical ocular drug delivery. *Clinic and Experiment Pharmacology and Physiology* 27:558-62.
- en Murciélagos E and Adultos R, 2009. Staining procedure of cartilage and skeleton in adult bats and rodents. *Int J Morphol* 27:1163-7.
- Garden O, Volk S, Mason N, *et al.*, 2018. Companion animals in comparative oncology: One Medicine in action. *Vet J* 240:6-13.
- Gelatt K, MacKay E, Widenhouse C, *et al.*, 2006. Effect of lacrimal punctal occlusion on tear production and tear fluorescein dilution in normal dogs. *Vet Ophthalmol* 9:23-7.
- Gilger BC, Abarca E and Salmon JH, 2014. Selection of appropriate animal models in ocular research: Ocular anatomy and physiology of common animal models. *Ocular Pharmacol and Toxicol* 5:7-32.
- Gilger BC, McLellan GJ, Michau TM, *et al.*, 2022. Editorial—Veterinary ophthalmology. Wiley Online Library, pp. 424-5.
- Hoffman AM and Dow SW, 2016. Concise review: stem cell trials using companion animal disease models. *Stem Cells* 34:1709-29.
- Johnston SA and Tobias KM, 2017. Eye. In: *Veterinary surgery: small animal expert consult-E-book*. 2nd Ed. Elsevier Health Sciences. pp:2341-69.
- Keller CB and Shilton CM, 2002. The amphibian eye. *Vet Clin: Exotic Anim Pr* 5:261-74.
- Kempster R, Bancroft B and Hirst L, 2002. Intraorbital anatomy of the koala (*Phascolarctos cinereus*). *The Anatomical Record: An Official Pub of the Am Ass of Anatomists* 267:277-87.
- Klećkowska-Nawrot J, Goździewska-Hartajczuk K and Nowaczyk R, 2016. Morphological study of the upper, lower and third eyelids in the African black ostrich (*Struthio camelus camelus* L., 1758) (Aves: Struthioniformes) during the embryonic and postnatal period. *Ital J Zool* 83:312-28.
- Klećkowska-Nawrot J, Marycz K, Czogała J, *et al.*, 2013. Morphology of the Lacrimal Gland and Superficial Gland of the Third Eyelid of Roe Deer (*Capreolus Capreolus* L.). *Paki Vet J* 33:139-44.
- Klećkowska-Nawrot JE, Goździewska-Hartajczuk K, Darska M, *et al.*, 2019. Microstructure of the eye tunics, eyelids and ocular glands of the Sulawesi bear cuscus (*Ailurops ursinus* Temminck, 1824) (Phalangeridae: Marsupialia) based on anatomical, histological and histochemical studies. *Acta Zoologica* 100:182-210.
- Kol A, Arzi B, Athanasiou KA, *et al.*, 2015. Companion animals: Translational scientist's new best friends. *Sci Trans Med* 7:308ps321-308ps321.
- König H, Liebich H, Korb R, *et al.*, 2007. Eye (organum visus). In: *Veterinary anatomy of domestic mammals: Textbook and colour atlas*. 3rd Ed. Stuttgart Publication. pp:571-93.
- Kumar MA, 2015. The Eye, Cranial nerves II, III, IV, VI. In: *Clinically oriented anatomy of the dog and cat*. 2nd Ed. Linus Learning Publication. pp:445-511.
- Lantyer-Araujo NL, Silva DN, Estrela-Lima A, *et al.*, 2019. Anatomical, histological and computed tomography comparisons of the eye and adnexa of crab-eating fox (*Cercopithecus thous*) to domestic dogs. *PLoS one* 14:e0224245.
- Ledbetter EC, Nicklin AM, Spertus CB, *et al.*, 2018. Evaluation of topical ophthalmic ganciclovir gel for the treatment of dogs with experimentally induced ocular canine herpesvirus-1 infection. *Amer J Vet Res* 79:762-9.
- Mazzucchelli S, Vaillant M, Wéverberg F, *et al.*, 2012. Retrospective study of 155 cases of prolapse of the nictitating membrane gland in dogs. *Vet Record* 170:443.
- Mohsen SM, Esfandiari E, Rabiei AA, *et al.*, 2013. Comparing two methods of plastination and glycerin preservation to study skeletal system after Alizarin red-Alcian blue double staining. *Adv Biomed Res* 2:19.
- Murphy C, Samuelson D, Pollock R, *et al.*, 2012. The Eye. *Miller's Anatomy of the Dog*. Ch. 21. Elsevier Saunders:746-85.
- Ofri R, Miller PE and Maggs DJ, 2008. THIRD EYELID. In: *Slatter's Fundamentals of Veterinary Ophthalmology*; 4th Ed. Elsevier Saunders:107-57.
- Oriá AP, Rebouças MF, Martins Filho E, *et al.*, 2018. Photography-based method for assessing fluorescein clearance test in dogs. *BMC Vet Res* 14:266-9.
- Park SA, Taylor KT, Zwingenberger AL, *et al.*, 2016. Gross anatomy and morphometric evaluation of the canine lacrimal and third eyelid glands. *Vet Ophthalmol* 19:230-6.

- Partridge B and Rossmeis J Jr JH, 2020. Companion animal models of neurological disease. *Journal of Neuroscience Methods* 331:108480-4.
- Pasza W, Klećkowska-Nawrot JE and Goździewska-Harłajczuk K, 2021. Anatomical and morphometric evaluation of the orbit, eye tunics, eyelids and orbital glands of the captive females of the South African painted dog (*Lycaon pictus pictus* Temminck, 1820) (Caniformia: Canidae). *Plos one* 16:e0249368.
- Pennington MR, Ledbetter EC and Van de Walle GR, 2017. New paradigms for the study of ocular alphaherpesvirus infections: insights into the use of non-traditional host model systems. *Viruses* 9:242-349.
- Schlegel T, Brehm H and Amselgruber W, 2001. The cartilage of the third eyelid: a comparative macroscopical and histological study in domestic animals. *Ann of Anatomy-Anatomischer Anzeiger* 183:165-9.
- Schober C, Teixeira L and Dubielzig R, 2013. The avian membrana nictitans: anatomy and function. *Inves Ophthalmol & Visual Sci* 54:6019
- Schramm U, Unger K and Keeler C, 1994. Functional morphology of the nictitating membrane in the domestic cat. *Ann of Anatomy-Anatomischer Anzeiger* 176:101-8.
- Sheehan D and Hrapchak B, 1980. *Theory and Practice of Histotechnology* (Mosby, St. Louis).
- Spencer L, Bancroft J, Bancroft J, et al., 2012. *Tissue processing. Bancroft's Theory and Practice of Histological Techniques*. 7<sup>th</sup> ed. Netherlands, Amsterdam: Elsevier Health Sci: 105-23.
- Vézina M, 2013. Comparative ocular anatomy in commonly used laboratory animals. *Assessing ocular toxicology in laboratory animals*: 1-21.